REPORT DOCUMENTATION PAGE

Form Approved OMB NO. 0704-0188

1. REPORT DATE (DD-MM-YYYY)	2. REPORT TYPE	3. DATES COVERED (From - To)
13-02-2014	Final Report	5-Feb-2011 - 4-Feb-2015

4. TITLE AND SUBTITLE
Final Report: BioComponent Robots

5a. CONTRACT NUMBER
W911NF-11-1-0079

5b. GRANT NUMBER

5c. PROGRAM ELEMENT NUMBER
0620BK

6. AUTHORS
David Kaplan, Barry Trimmer

5d. PROJECT NUMBER

5e. TASK NUMBER

5f. WORK UNIT NUMBER

7. PERFORMING ORGANIZATION NAMES AND ADDRESSES
Tufts University
Office of the Vice Provost
20 Professors Row
Medford, MA 02155 -5807

8. PERFORMING ORGANIZATION REPORT NUMBER

9. SPONSORING/MONITORING AGENCY NAME(S) AND ADDRESS (ES)
U.S. Army Research Office
P.O. Box 12211
Research Triangle Park, NC 27709-2211

10. SPONSOR/MONITOR'S ACRONYM(S)
ARO

11. SPONSOR/MONITOR'S REPORT NUMBER(S)
59657-MS-DRP.5

12. DISTRIBUTION AVAILIBILITY STATEMENT
Approved for Public Release; Distribution Unlimited

13. SUPPLEMENTARY NOTES
The views, opinions and/or findings contained in this report are those of the author(s) and should not contrued as an official Department of the Army position, policy or decision, unless so designated by other documentation.

14. ABSTRACT
The project goal was to exploit insect cell culture and tissue engineering approaches to generate biological actuators, utilizing the unique hardiness and longevity of insect cell sources for device applications for robotics. In contrast to mammalian cells and tissues, insect cells survive with minimal assistance over long periods of time and are immune to routine environmental perturbations. The project focused on 3 tasks: 1) cell-based actuators and biostability, 2) energy storage and conversion, and 3) tissue engineering. All phases of the project required new methods in order to move forward and significant progress was made on the three tasks. Cell sources from insects

15. SUBJECT TERMS
cell-based actuators, biostability, robot, elastomer films, silk, fibroin, thin films

16. SECURITY CLASSIFICATION OF:			17. LIMITATION OF ABSTRACT	15. NUMBER OF PAGES	19a. NAME OF RESPONSIBLE PERSON
a. REPORT	b. ABSTRACT	c. THIS PAGE			David Kaplan
UU	UU	UU	UU		19b. TELEPHONE NUMBER 617-627-3251

Report Title

Final Report: BioComponent Robots

ABSTRACT

The project goal was to exploit insect cell culture and tissue engineering approaches to generate biological actuators, utilizing the unique hardiness and longevity of insect cell sources for device applications for robotics. In contrast to mammalian cells and tissues, insect cells survive with minimal assistance over long periods of time and are immune to routine environmental perturbations. The project focused on 3 tasks: 1) cell-based actuators and biostability, 2) energy storage and conversion, and 3) tissue engineering. All phases of the project required new methods in order to move forward and significant progress was made on the three tasks. Cell sources from insects were isolated, cultivated, grown to confluence and beating muscle assemblies were generated and demonstrated forces comparable to bioengineered mammalian muscle systems. These systems were grown for at least three months without feeding or special handling. Metabolic studies characterized the carbon fluxes from the cells to provide insight into the role of adipose reserves in supporting cell functions. Studies related to anchoring the actuators and organizing multi-actuator systems, including the use of extracellular matrix components from the caterpillar body wall, were studied for generating functional assemblies. The project was terminated early due to funding constraints.

Enter List of papers submitted or published that acknowledge ARO support from the start of the project to the date of this printing. List the papers, including journal references, in the following categories:

(a) Papers published in peer-reviewed journals (N/A for none)

Received		Paper
09/05/2012	4.00	Guokui Qin, Xiao Hu, Peggy Cebe, David L. Kaplan. Mechanism of resilin elasticity, Nature Communications, (08 2012): 0. doi: 10.1038/ncomms2004
09/05/2012	3.00	Amanda L. Baryshyan, William Woods, Barry A. Trimmer, David L. Kaplan, Christophe Egles. Isolation and Maintenance-Free Culture of Contractile Myotubes from Manduca sexta Embryos, PLoS ONE, (02 2012): 0. doi: 10.1371/journal.pone.0031598
TOTAL:	**2**	

Number of Papers published in peer-reviewed journals:

(b) Papers published in non-peer-reviewed journals (N/A for none)

Received		Paper
TOTAL:		

Number of Papers published in non peer-reviewed journals:

(c) Presentations

Number of Presentations: 0.00

Non Peer-Reviewed Conference Proceeding publications (other than abstracts):

Received	Paper

TOTAL:

Number of Non Peer-Reviewed Conference Proceeding publications (other than abstracts):

Peer-Reviewed Conference Proceeding publications (other than abstracts):

Received	Paper

TOTAL:

Number of Peer-Reviewed Conference Proceeding publications (other than abstracts):

(d) Manuscripts

Received		Paper
09/04/2012	2.00	Xiao Hu, Peggy Cebe, David Kaplan, Guokui Qin. Mechanism of resilin elasticity, Nature Communications (10 2011)

TOTAL: **1**

Number of Manuscripts:

Books

Received Paper

TOTAL:

Patents Submitted

N/A

Patents Awarded

N/A

Awards

N/A

Graduate Students

NAME	PERCENT_SUPPORTED	Discipline
Amanda Baryshyan	1.00	
Emily Pitcam	0.40	
Fallon Schuler	0.40	
Michael Doire	0.10	
Amy Hopkins	0.50	
Erica Palma	0.40	
Lee Tien	0.60	
FTE Equivalent:	**3.40**	
Total Number:	**7**	

Names of Post Doctorates

NAME	PERCENT_SUPPORTED
Xiaoxia Xia	0.80
Laura Domigan	0.20
Vivesh Vikas	0.30
Jelena Rnjak	0.10
FTE Equivalent:	**1.40**
Total Number:	**4**

Names of Faculty Supported

NAME	PERCENT_SUPPORTED	National Academy Member
Barry Trimmer	0.10	
William Woods	0.30	
FTE Equivalent:	**0.40**	
Total Number:	**2**	

Names of Under Graduate students supported

NAME	PERCENT_SUPPORTED	Discipline
Wesley Field	0.01	Biology
Bassel Ghadder	0.01	Chemical Engineering
Bentley Hunt	0.01	Biomedical Engineering
Ryan Pandya	0.01	Chemical Engineering
Carolyn Saund	0.01	Computer Science
Brandon Wheeler	0.01	Biomedical Engineering
Kelly Banks	0.01	Biopsychology
Samuel Vaughn	0.01	Engineering
Nikita Saxena	0.01	Biomedical Engineering
Carter Palmer	0.01	Biomedical Engineering
Jordan Skeens	0.01	Biology
FTE Equivalent:	**0.11**	
Total Number:	**11**	

Student Metrics

This section only applies to graduating undergraduates supported by this agreement in this reporting period

The number of undergraduates funded by this agreement who graduated during this period:	2.00
The number of undergraduates funded by this agreement who graduated during this period with a degree in science, mathematics, engineering, or technology fields:	2.00
The number of undergraduates funded by your agreement who graduated during this period and will continue to pursue a graduate or Ph.D. degree in science, mathematics, engineering, or technology fields:	0.00
Number of graduating undergraduates who achieved a 3.5 GPA to 4.0 (4.0 max scale):	0.00
Number of graduating undergraduates funded by a DoD funded Center of Excellence grant for Education, Research and Engineering:	0.00
The number of undergraduates funded by your agreement who graduated during this period and intend to work for the Department of Defense	0.00
The number of undergraduates funded by your agreement who graduated during this period and will receive scholarships or fellowships for further studies in science, mathematics, engineering or technology fields:	0.00

Names of Personnel receiving masters degrees

NAME
Total Number:

Names of personnel receiving PHDs

NAME
Total Number:

Names of other research staff

NAME	PERCENT_SUPPORTED
FTE Equivalent:	
Total Number:	

Sub Contractors (DD882)

Inventions (DD882)

Scientific Progress

See attachment

Technology Transfer

FINAL PROGRESS REPORT
Reporting Period: February 2011 – July 2013

Program Overview – 3 TASKS:

Task 1 – Cell-Based Actuators and Biostability
- Cell isolation/characterization/nutrients
- Cell organization/alignment
- Force measurements
- Integration into systems
- Cell tolerance
- Cell immortalization, storage, utility
- Novel cell sources

Task 2 – Energy Storage and Energy Conversion
- Fuel sources
- Conversion efficacy
- Integration with cells with devices
- Packaging and placement in the systems
- Extreme biofuels and utility

Task 3 – Tissue Engineering – Growing a Robot
- Scaffold and anchoring needs
- Decellularized scaffolds
- Cell factors
- Tissue growth, interactions cells/matrices
- Platform design
- Bioreactor design

Task 1 – Cell-Based Actuators and Biostability – 3D printed seeding chambers

Approach
- We were able to produce 3D constructs (Figure 1) in a range of formats. For ease of scale-up and also to increase the consistency of the resulting constructs we have produced 3D printed molds for the seeding chambers used to generate a range of construct formats.

Advantages
- Molds were constructed such that they produce PDMS seeding chambers of optimal dimensions to favor cellular alignment and therefore maximize force output.
- Mold arrays allowed for easy scale up and reproducibility of the resulting construct.

Results
- Seeding chamber molds were designed using SolidWorks and then 3D-printed. These molds were used to produce PDMS seeding chambers which were used to produce 3D constructs in a reproducible and high throughout manner.

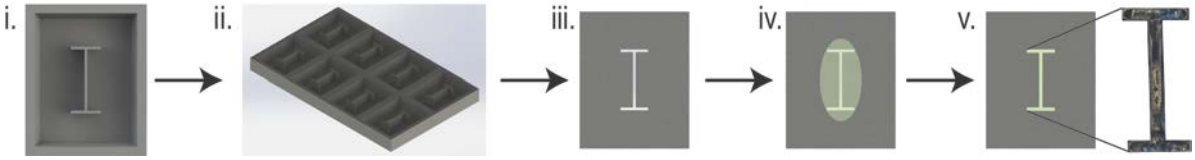

Figure 1. Formation of 3D scaffold free muscle constructs. Seeding chamber molds were designed to the desired dimensions using SolidWorks (i), and arrays of these 3D printed (ii). PDMS was cast into the mold arrays (iii) and a high density cell suspension dropped on top of the chamber (iv). Contractile 3D constructs were then allowed to develop over time (v). A phase contrast image of one such construct is shown in the inset.

Task 1 – Cell-Based Actuators and Biostability – Construct self-healing

Approach

- We grew muscle constructs and after 14 days of cultivation, we resected a 1-mm segment of each construct, creating a 1-mm long defect (Figure 2). This defect served to mimic major damage to the construct, which might occur during operation. We then acquired microscopy images of cells migrating into and repairing the defect every few days.

Advantages

- Mammalian muscle tissue does not fully repair itself when a large segment is removed. Rather, fibrous, noncontractile tissue tends to fill the wound.
- We have several cell types present in our system, including a population of muscle stem cells that remain throughout the duration of the culture. Furthermore, these cells are attracted to corresponding, "tendon-like" cells also likely present in our cultures. The attractive factors from the tendon cells cause the developing muscle to grow and reach toward the tendon cells. We believe the phenomenon may be occurring in our self-healing cultures, as developing muscle in the defect stretches and reaches toward the other side.

Results

- After injuring constructs, we found cells migrating into the wound area and reaching toward the other side. The cells continued migrating and reaching until the gap was bridged, and contraction was observed in the wound area.

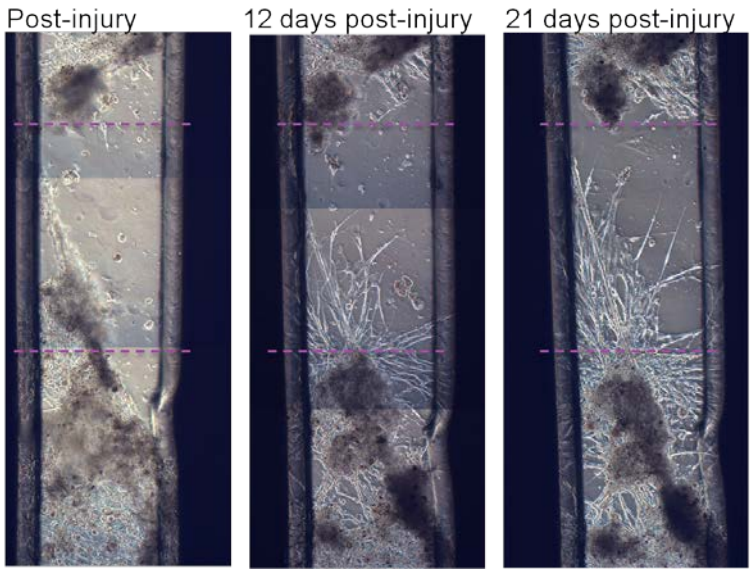

Figure 2. Construct self-healing after 1-mm segment removed. 2-week old constructs were subjected to major injury by removing a 1-mm tissue segment. Subsequently, cells were observed to migrate into the wound, fuse and form new muscle fibers. By 21 days post-injury, the wound area had nearly been filled with new cells.

Task 1 – Cell-Based Actuators and Biostability – Long-term construct survival

Approach

- We demonstrated that insect cells can survive for long periods of time in the absence of medium replenishment in 2 dimensional monolayers (Baryshyan *et. al.*, 2012), but we wanted to confirm that, even in dense 3-dimensional structures, our cells continued to survive for extended time periods.
- We grew constructs for 90 days, then stained the cells using a LIVE/DEAD kit, which results in live cells appearing green, and dead cells appearing red.

Advantages

- The transition from 2D to 3D allowed for greater force production, handleability and versatility of our system. Several groups have already demonstrated cell bioactuation in 2D, as 3D tissues are more difficult to keep alive. Nutrient diffusion into the center of the tissue is often limited and since a vascular system is usually absent in *in vitro*-cultured tissues, the center of the construct usually dies
- Insect cells were more tolerant of low oxygen conditions, in addition to their ability to survive without nutrient replenishment, thus the limitations of 3D bioactuators may not apply to insect cells.

Results

- After 3 months of culture, the viability of cells throughout the construct remained high (Figure 3).
- Muscle cells can be observed forming dense networks of viable cells, indicated by green coloration.

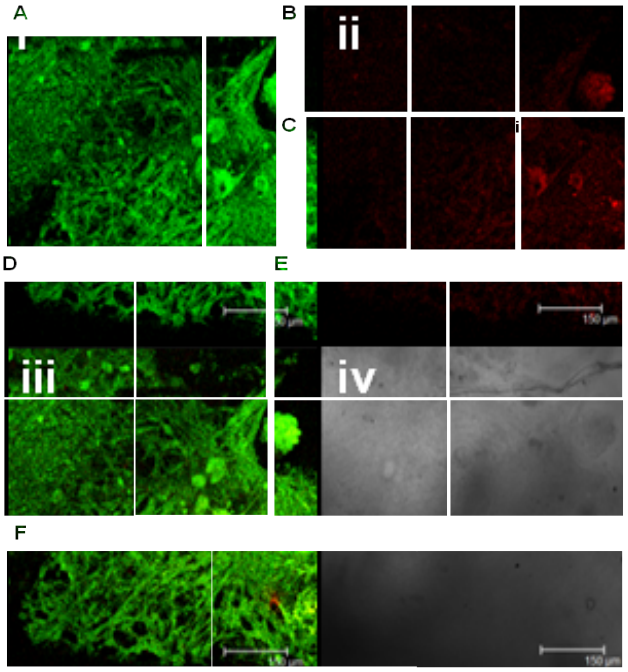

Figure 3. Long-term survival of insect muscle constructs. LIVE/DEAD staining and confocal imaging reveals viability of cells throughout the thickness of the construct. Live cells are stained green (**i**), dead cells appear red (**ii**). Both live and dead cells are overlain in panel **iii**. Panel **iv** shows phase contrast image of construct.

Task 1 – Cell-Based Actuators and Biostability – Construct environmental tolerance

Approach

- We used index of movement analysis to look at the contractile activity of 2 month old constructs at their normal culture temperature and at human body temperature. Videos were collected and frames were analyzed at 600ms intervals. Each frame was normalized to the first frame of the video, and 8 normalized images were stacked to generate the pseudocolored images.
- The resulting images therefore represent a 4.8 second time period, where brighter coloration indicates regions where pixel values changed the most, and therefore indicates regions of spontaneous contractions during the 4.8s sampling time.

Advantages

- Mammalian cells are cultured at body temperature, which is 37°C. At any other temperature, these cells rapidly die.

- Insect cells were cultured at ambient temperature, usually 26°C, since they are not warm-blooded. However, for future applications of our technology, and to demonstrate the extreme versatility of our system, we wanted to culture our cells at body temperature as well, and to evaluate their contractile activity after being exposed to 37°C for 24 hours.

Results

- Cells analyzed after culture at 26°C contracted spontaneously as expected.
- After incubating the constructs for 24 hours at body temperature, spontaneous contractions persisted and even increased. Though there was a qualitative increase in activity at higher temperatures, this change was not significant (data not shown).

Task 1 – Cell-Based Actuators and Biostability – Characterizing spontaneous contractile activity

Approach

- In the past, we have shown contractile activity of muscle constructs using indirect methods, such as index of movement analysis.
- We also wanted to demonstrate and quantify force production using direct methods, such as force measurement with a force transducer system.

Advantages

- Using a sensitive, custom-built force transducer setup, we analyzed spontaneous contractions, including stress in kPa. Furthermore, our data reveals frequency and duration of contractions (Figure 4).

Results

- Spontaneous contractions, usually occurring as double-peaks, were observed with a stress of approximately 2kPa. The duration of double-peak contractions was around 4 seconds, and occurred with irregular frequency.

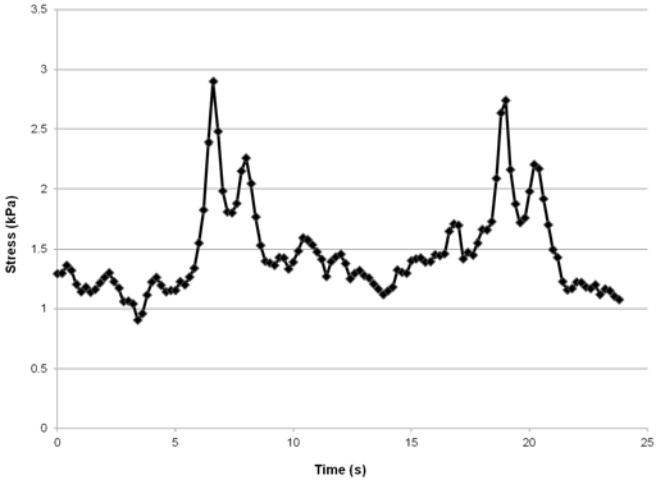

Figure 4. Force data from spontaneous construct contractions.

Task 2 – Energy Storage and Energy Conversion – Metabolic needs of 3D actuators

Approach

- We previously showed that contracting 2D cultures of *M. sexta* myoblasts did not require media changes in order to survive, and that they do not consume glucose – unlike their mammalian counterparts (Baryshyan *et al.* 2012).
- The metabolic needs of contractile 3D actuators were assessed. 3D constructs were seeded and allowed to develop into contractile structures over a period of one month. At this point, the media was replaced and various metabolites assayed over a 10 day period, during which contraction was sustained.

Advantages

- Knowledge of the metabolic requirements of contractile 3D actuators enabled us to ensure that the chosen fuel source is one which can adequately meet these requirements whilst the actuator is functioning.

Results

- Extracellular glucose, protein and triglyceride assays were carried out and no deletion was seen over the duration of the experiment.
- This indicated that the cells were not relying on any of these fuel sources, supporting earlier hypotheses that the presence of yolk cells is sufficient to fuel the contraction of these cells.
- Confocal imaging of constructs stained for muscle (green) and lipid droplets (red) verified the presence of lipid-containing cells, which could be responsible for the production of nutrients and extended construct survival.

Task 3 – Growing a robot – Muscular thin film actuators

Approach

- As has been previously shown in the literature, muscular thin film actuators have wide applicability in robotics, either as free standing contractile structures or as a component of a robot body wall.
- In contrast to previous work which has used thin silicone films, our approach was to use a biological material, namely silk fibroin.
- Flexible and insoluble thin films were formed by blending silk fibroin with glycerol (30% dry weight) and casting films into well plates.
- In order to promote cell adhesion, a number of coatings were applied to the silk-glycerol films. These included fibronectin, laminin, CellTak™, ECM extract (obtained from decelluarised *M. sexta* larvae), and RGD peptide.
- Muscle precursor cells were seeded and differentiated into mature muscle cells using 20-HE (Figure 5).
- We developed a customized 3D printer which is able to print silk-glycerol films down to a thickness of 5 µm. We used silk-glycerol films in various simple shapes which were then seeded with muscle cells in order to generate contractile structures. In future work, this technology can be used to print more complex structures.

Advantages

- Silk fibroin is a biocompatible and biodegradable material.
- Silk-glycerol films have been previously shown to be more elastic than silk films
- 3D printing technology allowed uniform printing of silk structures in a range of formats and dimensions.

Results

- Cell growth was observed under all conditions examined (Figure 10).

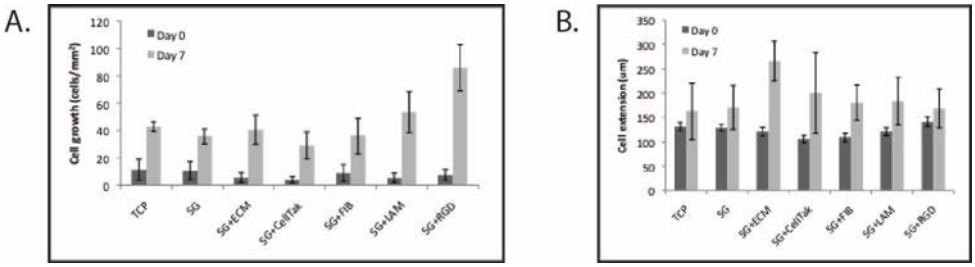

Figure 5. Graph showing cell growth (cells/mm²) on silk-glycerol films coated with a range of coatings intended to promote cell adhesion.

- After 3 months in culture, dense network structures were present, with mature muscle cells observed to fuse into larger myotubes. Yolk and epithelial cells were also observed in these cultures which contributed to their sheet-like appearance.
- Contraction was observed in cultures from Day 7, and by 3 months in culture contraction of whole cell "sheets" was seen (Figures 6, 7).

- SG films with cells could be handled with whole cell sheets able to be removed from the well-plate where they were cast and placed in a new culture dish. The cells continued to grow and contract when on a free-standing film.
- Silk-glycerol films were printed in simple shapes and these were seeded with muscle precursor cells. Cells were seen to differentiate on the print shapes and contractions observed.

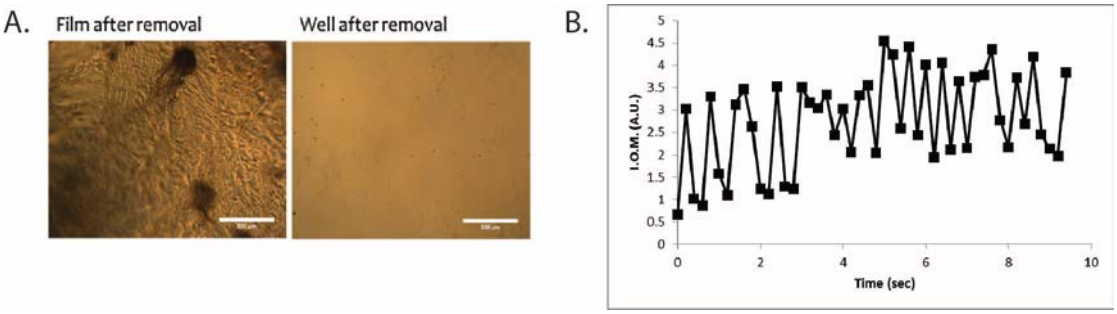

Figure 6. After 3 months in culture, silk-glycerol films with contractile muscle cells were removed from the 24 well plate where they were seeded and transferred to a petri dish. The cells remained on the film (A), and continued to contract (B).

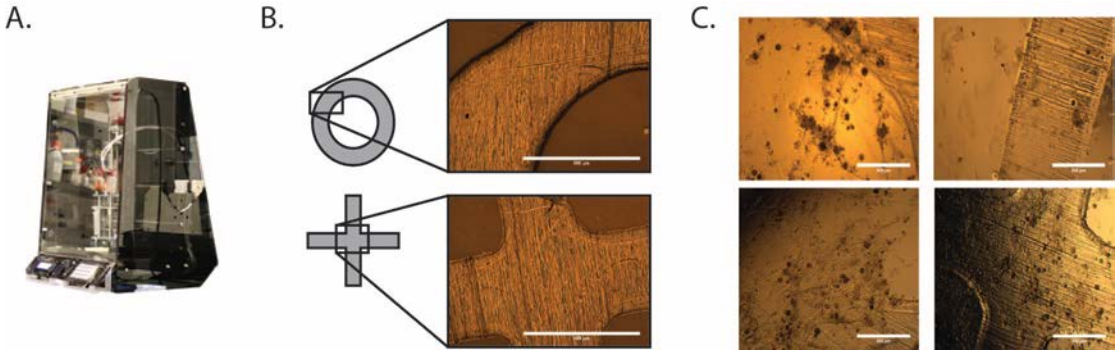

Figure 7. A customised in-house 3D printer (A) was used to print simple shapes comprised of silk-glycerol films (B). These shapes were then seeded with muscle precursor cells and they cells seen to develop and contract (C).

Summary of Findings (draft publication):

<u>Insect muscle bioactuators with long term function and under ambient conditions</u> (note, Figures and videos omitted here for space)

Abstract: Long term functioning insect cell-based bioactuators were generated with significant enhancements in environmental tolerance. Mammalian cell-derived muscle bioactuators lack function at room temperature and can not be fabricated for multiple device dimensions with long term function. To address this need, insect muscle stem cells were used as the biological source material from which to generate muscle tissues as organized 3D structures. These tissues self-assembled, self-repaired, survived for months in culture without media replenishment and produced stresses of up to 2 kPa, all under ambient conditions. When temperature and pH conditions were further stressed to supraphysiological levels, the muscle tissues continued to function for days. Furthermore, the dimensions and geometry of these tissues can be easily scaled to MEMS or meso-scale devices. The versatility, environmental hardiness and long term function provide a new path forward for biological actuators for device needs.

In recent years, muscle tissue engineering has been explored for applications beyond the field of regenerative medicine, including as biological motors or bioactuators, and for microelectromechanical systems (MEMS) (*2, 3*) and robotic devices (*4*). Tissue engineering approaches with mammalian cardiac or skeletal muscle cells have been explored to devise muscle structures with potential as bioactuators. For example, gel-mediated cell condensation around micropillars, microcontact printing of flexible membranes, and poly(N-isopropylacrylamide) (PIPAAm)-released cell sheets have been employed to generate structures that can perform deflection, curling or pumping actions, respectively (*6, 7, 8*). Crawling- and swimming-type locomotions have also been demonstrated with free-standing devices (*9, 10*). These strategies can provide a range of bio-mimetic motion and simplify the manufacture of micro-scale actuators by exploiting the ability of cells to self-assemble and to coordinate contraction and function. Furthermore, cell-based bioactuators may have utility over synthetic systems due to the potential for self-repair, tunable biodegradability, and biocompatible fuel sources such as sugars and fats). However, a major limitation to the above systems comprised of mammalian cells are the stringent controls of temperature, pH, and oxygen for survival and function.

As an alternative, explanted insect tissues maintained at ambient temperatures and withstand a range of pH and oxygen conditions have been studied. However, these explants are restricted in dimensions, organization and lifetime. Furthermore, the use of excised tissues requires dissection for each device, limiting scalability and leading to poor reproducibility.

In the present study, we used a bottom-up bioengineer approach with insect muscle bioactuators, generating free-standing 3D muscle tissues from embryonic *M. sexta* muscle stem cells. The goal was to mimic the simple structure of insect muscle and retain desirable properties of the native tissues (Fig. 1A), along with resistance to environmental perturbations. The insect cell systems displayed several distinguishing characteristics not achievable with mammalian cell systems. For example, the muscle cells self-assembled into 3D structures without the need to be embedded in a hydrogel or other extracellular matrix (ECM) materials (Fig. 1A). The tissues were comprised of muscle cells through the influence of the insect hormone 20-hydroxyecdysone (20-HE) supplementation in the growth media, as shown by positive myosin staining (Fig. S1). However, given that the entire contents of the developing embryo were used to generate these tissues, other cell types contributed in a positive mode to the structure and function. The ability of the tissue to form without supplementary ECM was due to production of matrix material by the cells (Fig. S2). For example, in *M. sexta* epithelial cells generate matrix for muscle cell insertion underlying the cuticle.

As the insect muscle tissues developed, spontaneous contractile activity was observed. Initially, individual cells and clumps of cells pulsed continuously (Fig 1Bi, Movie S1). This activity slowed after two weeks, presumably due to cell fusion and muscle network formation (Fig. 1Bii, Movie S2). Spontaneous contractile activity significantly increased from day 21 to day 30; with the entire tissue construct contracting in a coordinated fashion. (Fig. 1C, Movie S3), and by day 30, the muscle tissue had condensed and formed a functional bioactuator unit (Fig. 1Biii). Force production of mature tissues (>d30) was assessed. Index of movement analysis was used for indirect measures of contractions, which allowed observations of the duration and relative amplitude of a contraction based on video analysis, but not the specific force. To measure forces, a custom-built piezoelectric force transducer was utilized (Fig. S3A – B). A representative trace from indirect measurements showed that contractions were typically 2 – 4 seconds in duration, and tended to display a double-peak (Fig. 1D). Direct measurements mirrored the peak duration and double-peak characteristics seen in the video analysis (Fig. S3C). The double-peak may be an indication of the presence of stretch-responsive fibers, or other physical or chemical connectivity within the network, such as cardiac muscle gap junctions or paracrine signaling. The individual contractions produced forces of around 2 kPa.

During insect myogenesis, developing muscle fibers reach out and are attracted to tendon-like cell precursors, which eventually anchor the muscle fibers to the larval body wall. We wanted to see if a similar process was possible *in vitro*, as this could lead to self-healing capabilities in the constructs, as

well as anchoring of bioactuators within devices. A 1-mm defect introduced into a preformed muscle partially repaired itself within one month, and contraction resumed in the repaired region (Figure 1E). Muscle cells grew into the defect and migrated toward the opposite side of the resected region. Slow migration of a few cells was initially observed and after 30 days, cell elongation and further migration resulted in a dramatic increase in defect repair, approximately 40% on average (Fig. 1F). Although this process took several weeks to complete, it could potentially be accelerated by chemically attracting muscle stem cells or by increasing the cellular organization within the constructs.

Insect muscle tissues were generated using a simple molding technique whereby cells were seeded and confined within polydimethylsiloxane (PDMS) chambers having open bottoms to allow cells to attach to underlying tissue culture plastic (TCP) (Fig. 2A). After sterilization, the chambers were placed on TCP dishes and dried. Cell suspensions were seeded within the chambers at a density of 1 embryo/mm^2 in a small volume of medium. Samples were flooded with medium after several days, and 3D muscle structures formed. Tissue size and geometry were controlled based on the shape and size of the PDMS chamber, such that I-bars, rings, and eyelets were generated (Fig. 2B). Different biomaterials can be incorporated as end points for anchoring by pre-placement in the chambers prior to cell seeding. Silk sutures and stainless steel pins were demonstrated (Fig. 2C). The cells grew around the structures as anchoring points and can then be used to secure the insect tissue construct to a device. For more complicated geometries, such as multifiber arrays, 3D printed inverse chambers were used as master molds for casting the PDMS chambers (Fig. 2D – E).

In order to effectively guide muscle cell alignment, and thereby maximize coordination and force output, the width of the chamber channels was optimized to 500μm to guide cellular alignment (Fig. S4). This corresponded to the dimensions of insect muscle fibers found *in vivo,* around 300μm in width, while individual native muscle fibers found *in vivo* are unicellular whereas the tissues generated in vitro are multicellular.

M. sexta muscle cells cultivated *in vitro* survive for several months in the absence of medium replenishment. Despite potential diffusion limitations in our 3D system, the *in vitro* cultured muscle tissues also thrived without changes in media over at least 90 days, with the majority of muscle cells were still viable by LIVE/DEAD staining (Fig. 3A). This result is in major contrast to mammalian cell systems, which require medium exchanges every 2 to 3 days to maintain viability. Three possible fuel sources, glucose, protein, and triglycerides, were assessed over a two-week period to elucidate the metabolic strategy used by these tissues to survive. The extracellular levels of these metabolites were not significantly depleted over this time period in mature, contracting tissues (Fig. 3B, Fig. S4). One possible explanation is *in vitro* production or mobilization of stored energy substrates by adipocyte or yolk cells present in the cultures, which resulted in maintainence of fuel despite energy use and end-product production (Fig. Sx). Yolk cells are maternally derived and are present from the initiation of the cultures. Adipocytes differentiate after muscle in the *M. sexta* embryo, but may develop within the cultures, and cells containing lipid droplets were present within the tissues grown in vitro (Figure 3C).

In addition to long-term, maintenance-free viability, another desirable feature of bioactuators is temperature tolerance and versatility. The spontaneous contractile activity of the muscle tissues at 26°C, close to room temperature; human body temperature (37°C); and 15°C were assessed. The insect muscle tissues displayed sustained contractions at all three temperatures with activity at 37°C and 15°C not significantly different from 26°C. Therefore, *M. sexta* bioactuators were excellent candidates for applications at fluctuating ambient temperatures, and at human body temperature. Contractile activity was also assessed at pH 5.5, 6.5, and 7.5 and sustained contractions were observed at all of these pH levels.

Metabolic analysis

Metabolism of the cells was assessed to determine substrates being used for energy, and to understand the extended survival of the insect cells *in vitro*, even in the absence of media replenishment. During embryonic development, maternally-derived yolk cells provide fuel to the developing embryo. In later

stages of development, the yolk cells are incorporated into the gut or ingested by the immature larva; however, fuel delivery in these systems is not well understood in the early stages of development. In the larval stage, the animal's diet is primarily responsible for supplying carbohydrates to provide energy for growth and foraging activity, while in the adult, fat cells may deliver fuel to the flight muscles in one of three forms, depending on the species. These forms include carbohydrates as the sugar trehalose, which is converted to glucose; and proline, which is metabolized to alanine. The third source, triglycerides, are metabolized to diacylglycerol, which is shuttled through the hemolymph to the muscle, where further metabolism leads to free fatty acids for energy in the mitochondria. The extracellular levels of glucose, protein, and triglycerides/diacylglycerol were assessed in the media of insect muscle cell cultures over time to identify the fuel source utilized in the tissues.

Materials and Methods

Cell isolation and seeding - Egg harvesting, culture medium preparation, and cell isolations were performed as previously described. All reagents were purchased from Invitrogen (Carlsbad, CA) or Sigma-Aldrich (St. Louis, MO), unless otherwise indicated. Briefly, eggs laid within a three hour period were collected from a *Manduca sexta* colony. The eggs were incubated for an additional 19 hours at 26°C. After 19 hours of incubation, embryos were counted, washed with dH_2O and sterilized in 25% bleach for 2 minutes. Embryos were then washed thoroughly with sterile water. Culture medium was prepared with 70% Leibovitz's L15 medium, 18% Grace's Insect Medium, 12% fetal bovine serum (FBS), 3.4 mg/mL yeast extract, 3.4 mg/mL lactalbumin hydrolysate (MP Biomedicals, Solon, OH), 0.37 mg/mL α-ketoglutaric acid, 1.21 mg/mL D (+)-glucose monohydrate, 0.67 mg/mL malic acid, 60 µg/mL succinic acid, 60 µg/mL imidazole, 1% Anti-Anti, 0.5% 1X RPMI 1640 vitamin mix, 0.5% 1X RPMI 1640 amino acid mix, and 20 ng/mL 20-hydroxyecdysone (20-HE). Medium was sterile filtered before use and the pH was adjusted to 6.5 with sterile 1M NaOH. The embryos were rinsed with media before transfer to a 7 mL Dounce homogenizer (Wheaton, Millville, NJ). Cells were released by lysing the embryos using plunger B. The homogenate was centrifuged twice, each for 5 minutes at 85 ×g to remove excessive yolk material and pellet the cells. The pellet was then resuspended in medium and plated at a density of 5 embryos/cm^2.

Immunofluorescence staining and imaging - Immunostained samples were prepared as described previously. Briefly, samples were fixed in 10% neutral buffered formalin (NBF), permeabilized in 1 wt% bovine albumin serum (BSA) and 0.05 wt% saponin, and blocked in 1 wt% BSA with 10% serum from the animal the secondary antibody was raised in. Samples were then incubated overnight at 4°C in primary antibody (Myosin 1:4). Samples were washed twice with PBS before incubation with secondary antibody and DAPI (1:1000 dilution). Samples were washed with PBS before visualizing using a Leica fluorescence microscope or confocal microscope.

Metabolic evaluation - Metabolic analyses were carried out on 30 day old constructs over a two week period. During the experimental period contraction was also monitored (see Contraction Evaluation) to ensure metabolic activity of actively contracting constructs was being captured. During the two week period media samples (60 µL from a total media volume of 2.5 mL) were taken at designated timepoints and glucose, protein, triglyceride and lactate concentrations assayed. Glucose assays were carried out using the Glucose (GO) Assay kit (Sigma). Protein assays were carried out using the BCA Protein Assay kit (Pierce). Triglyceride assays were carried out using the EnzyChrom Triglyceride Assay kit (BioAssay Systems, Hayward, CA). Extracellular lactate was evaluated using the EnxyChrom L-Lactate Assay kit (BioAssay Systems, Hayward, CA). All metabolic assays were carried out in 96-well plates using a plate reader (Molecular devices SpectraMax M2) according to the manufacturer's protocols.

LIVE/DEAD staining and imaging - Cultures were initiated using the methods described above. At designated time points, cultures were stained using a LIVE/DEAD kit, according to the manufacturer's instructions.

Environmental tolerance - After two weeks of culture at 26°C, videos were acquired for all experimental constructs to record spontaneous contractions. 3 videos were taken per construct at 10X magnification and 1280 x 960 pixel resolution. Video frames were captured at 600ms intervals, and 8 frames were acquired for each video. Samples were either replaced at 26°C, or switched to a humidified incubator at 37°C or 15°C. For samples where pH was being investigated, media was replaced with media that had been adjusted to the appropriate pH (5.5, 6.5, 7.5) and samples maintained at 26°C. Negative controls were constructs fixed in 10% NBF for 45 minutes at room temperature. At each timepoint, videos were again acquired from each construct and used for index of movement (IOM) analysis. IOM analysis was performed as described previously using ImageJ. To generate pseudocolored images, the first frame from each video was subtracted from the remaining seven to generate seven absolute value images. These were then added together to create a single differential image, which was then pseudocolored on a scale from 0 to 256. The areas of the pseudocolored images with the highest values correspond to the regions where the greatest change in pixel intensity, and therefore the most movement, occurred during the 4.8s video. For IOM quantification, average pixel intensity for each absolute value image was quantified and summated to generate a single IOM value for that video. IOM values were averaged across 3 videos per construct, and the mean and standard deviation for each condition was calculated.

Chamber preparation - Hand-cut seeding chambers were prepared by first generating a template using a drawing software package such as Solidworks. The design was printed on an ink-jet printer and taped face-up to the bottom of a Petri-dish that had previously been coated with a thin layer of Sylgard 184 silicone elastomer (Dow Corning, Midland, MI), according to the manufacturer's instructions. Under a dissecting microscope, the shape specified by the printed template was cut out using an Exacto knife or similar instrument. The chambers were then sterilized in ethanol and washed twice in PBS prior to cell seeding. 3D printed master molds for casting PDMS chambers were fabricated by designing molds using the CAD software Solidworks. The designs were printed using an Objet Connex500 3D printer with the Objet VeroClear™ material. The printed templates were thoroughly washed with water to remove the support material. The molds were dried and coated with Mann Ease Release 200 mold release spray. Sylgard 184 silicone elastomer (PDMS, Dow Corning, Midland, MI) was prepared according to the manufacturer's instructions. Approximately 1 g per mold of uncured silicone elastomer was added to each mold. The molds were degassed in a vacuum chamber prior curing at 60° C for 6 hours. The chambers were then removed and further modifications such as filters for further yolk removal or addition of silk sutures carried out where desired. For filter incorporation two holes are made at the ends of the channels using a size 3-biopsy punch. Nylon net filters with 10 um pores are cut to fit over the holes. The filters are fixed in place by DAP 100% Silicone Adhesive to create a watertight seal around the filter. Ethanol sterilized silk sutures are placed approximately 1 cm apart in culture dish. The PDMS chambers are placed over the sutures. The PDMS chambers are sterilized with 70% ethanol overnight and washed with sterile PBS for 48 hours. Remaining PBS is aspirated from and around the PDMS channels to secure the channels to the dish.

Contraction evaluation - Indirect tracking of spontaneous contractions were performed using IOM analysis, as described above.Direct measurements of spontaneous contraction force were measured using a custom-made force transducer setup.

Statistics - All assays were performed with a minimum sample size of n=3. Experimental groups were compared using a two-sided Student's t-test in Microsoft Excel. Statistically significant values are defined as indicated.

References and Notes:

1. L. Ricotti, A. Menciassi, Bio-hybrid muscle cell-based actuators. *Biomed. Microdevices* **14**, 987 – 998 (2012). (Review)
2. H. Fujita, V. T. Dau, K. Shimizu, R. Hatsuda, S. Sugiyama *et. al.*, Designing of a Si-MEMS device with an integrated skeletal muscle cell-based bio-actuator. *Biomed. Microdevices* **13**, 123 – 129 (2011).
3. E. Choi, S. Q. Lee, T. Y. Kim, H. Chang, K. J. Lee *et. al.*, MEMS-based power generation system using contractile force generated by self-organized cardiomyocytes. *Sens. Actuators, B* **151**, 291 – 296 (2010).
4. Y. Akiyama, T. Sakuma, K. Funakoshi, T. Hoshino, K. Iwabuchi *et. al.*, Atmospheric-operable bioactuator powered by insect muscle packaged with medium. *Lab Chip* **13**, 4870 – 4880 (2013).
5. You can use a numbered list in Word.
6. T. Hoshino, K. Imagawa, Y. Akiyama, K. Morishima, Cardiomyocyte-driven gel network for bio mechano-informatic wet robotics. *Biomed. Microdevices* **14**, 969 – 977 (2012).
7. A. W. Feinberg, A. Feigel, S. S. Shevkoplyas, S. Sheehy, G. M. Whitesides *et. al.*, Muscular thin films for building actuators and powering devices. *Science* **317**, 1366 – 1370 (2007).
8. Y. Tanaka, K. Soto, T. Shimizu, M. Yamato, T. Okano *et. al.*, A micro-spherical heart pump powered by cultured cardiomyocytes. *Lab Chip* **7**, 207 – 212 (2007).
9. V. Chan, K. Park, M. B. Collens, H. Kong, T. A. Saif *et. al.*, Development of miniaturized walking biological machines. *Sci. Rep.* **2**, 857 – 864 (2012).
10. J. C. Nawroth, H. Lee, A. W. Feinberg, C. M. Ripplinger, M. L. McCain *et. al.*, A tissue-engineered jellyfish with biomimetic propulsion. *Nat. Biotech.* **30**, 792 – 797 (2012).
11. R. Luedeman, R. B. Levine, Neurons and ecdysteroids promote the proliferation of myogenic cells cultured from the developing adult legs of *Manduca sexta*. *Dev. Biol.* **173**, 51 – 68 (1996).
12. Y. Yamahama, K. Seno, T. Hariyama, Changes in lipid droplet localization during embryogenesis of the silkworm, *Bombyx mori*. *Zool. Sci.* **25**, 580 – 586 (2008).
13. Sdlfjsjkh
14. Fdskjhfk
15. Sdkfhksjh
16. N. H. Haunerland, Transport and utilization of lipids in insect flight muscles. *Comp. Biochem. Physiol.* **117B**, 475 – 482 (1997).